Electronic Supplementary Material (ESI) for Catalysis Science & Technology.

Supporting Information

Remote Ion-Pair Interactions in Iron Porphyrin-Based Catalysts for the Hydrogen Evolution Reaction

Sitthichok Kasemthaveechok, Bruno Fabre, Gabriel Loget,* Rafael Gramage-Doria*

Univ Rennes, CNRS, ISCR-UMR 6226, F-35000 Rennes, France

gabriel.loget@univ-rennes1.fr; rafael.gramage-doria@univ-rennes1.fr

Contents *Page*

S1. Additional electrochemical data S3

S2. Detailed study of iron-based porphyrin 4. S8

S3. UV-vis titration studies of **1**-**4** and **2'**-**4'** with Et_3NHCl S11

S4. Computational study S15

S5. Plausible mechanism S20

S6. NMR Spectra S21

S7. References S25

S1. Additional electrochemical data

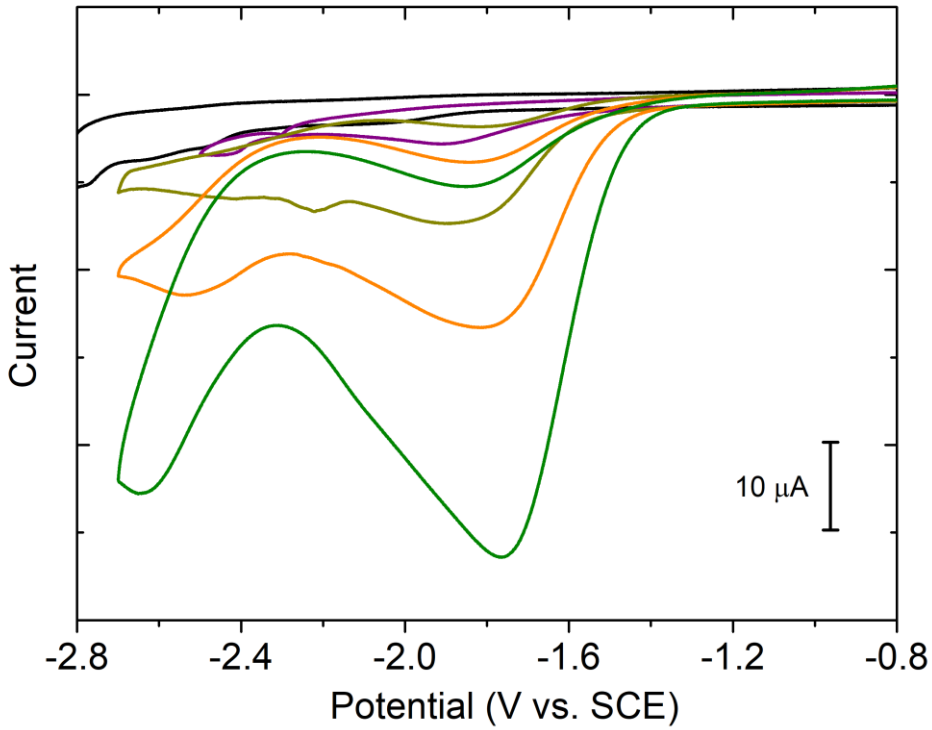

Figure S1. CVs of 0 mM (— Black), 1 mM (— Purple), 2.5 mM (— Dark Brown), 5 mM (— Orange) and 10 mM (— Green) solutions of Et_3NHCl in DMF (0.1 M $[Bu_4N^+][PF_6^-]$) at 100 mV s^{-1}. *The reduction peak corresponds to the reduction of Et_3NHCl in the absence of iron catalyst.*

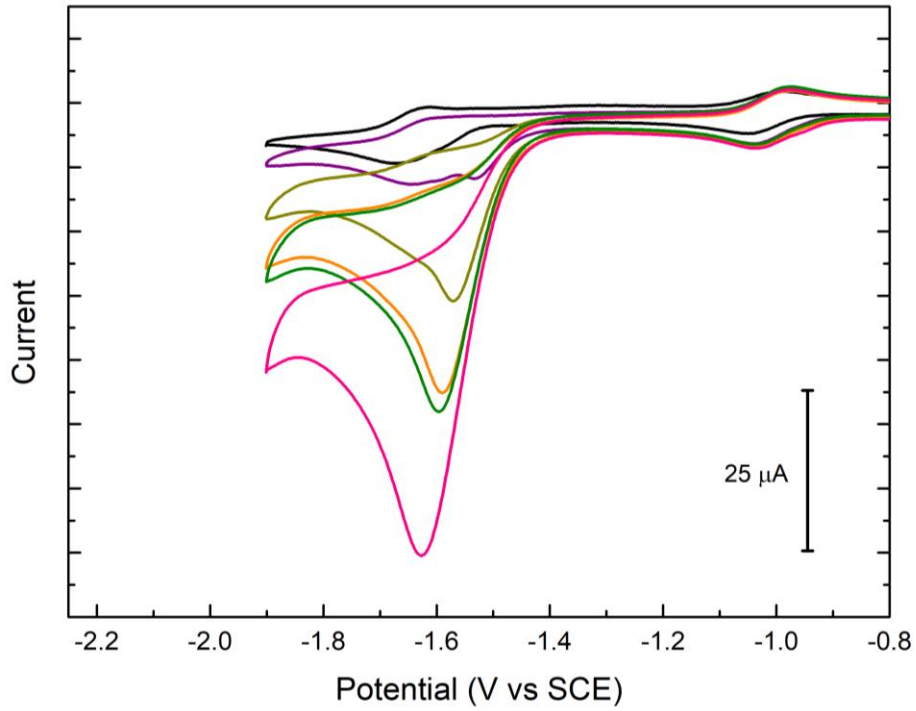

Figure S2. Cyclic voltammograms of **1** (0.5 mM) in the presence of 0 mM (— Black), 1 mM (— Purple), 2.5 mM (— Dark Brown), 5 mM (— Orange), 7.5 mM (— Green), 10 mM (— Pink) Et_3NHCl in DMF (0.1 M $[TBA^+][PF_6^-]$) at 100 mV/s.

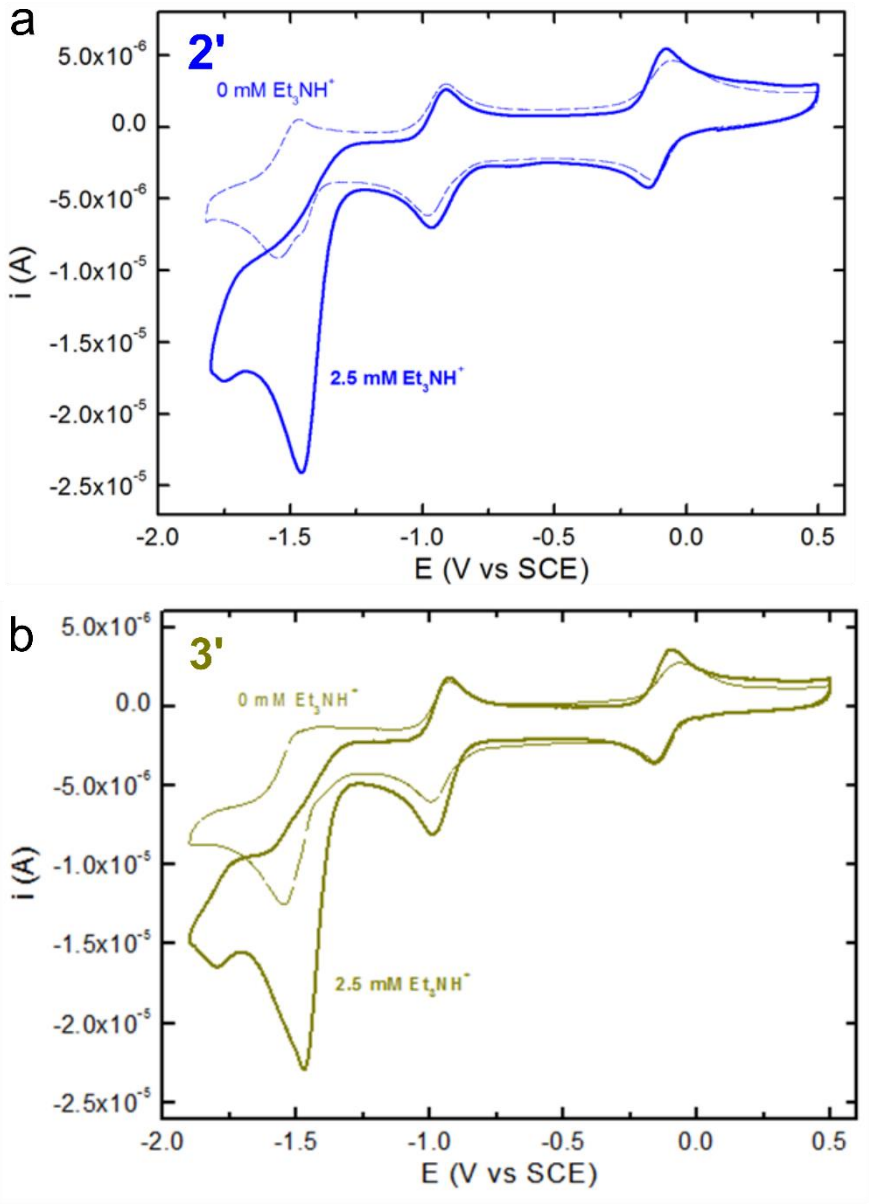

Figure S3. CVs of 0.5 mM **2'** (a) and **3'** (b) in the absence (dashed) and in the presence (solid lines) of 2.5 mM Et_3NHCl in DMF (0.1 M $[Bu_4N^+][PF_6^-]$) at 100 mV s^{-1}.

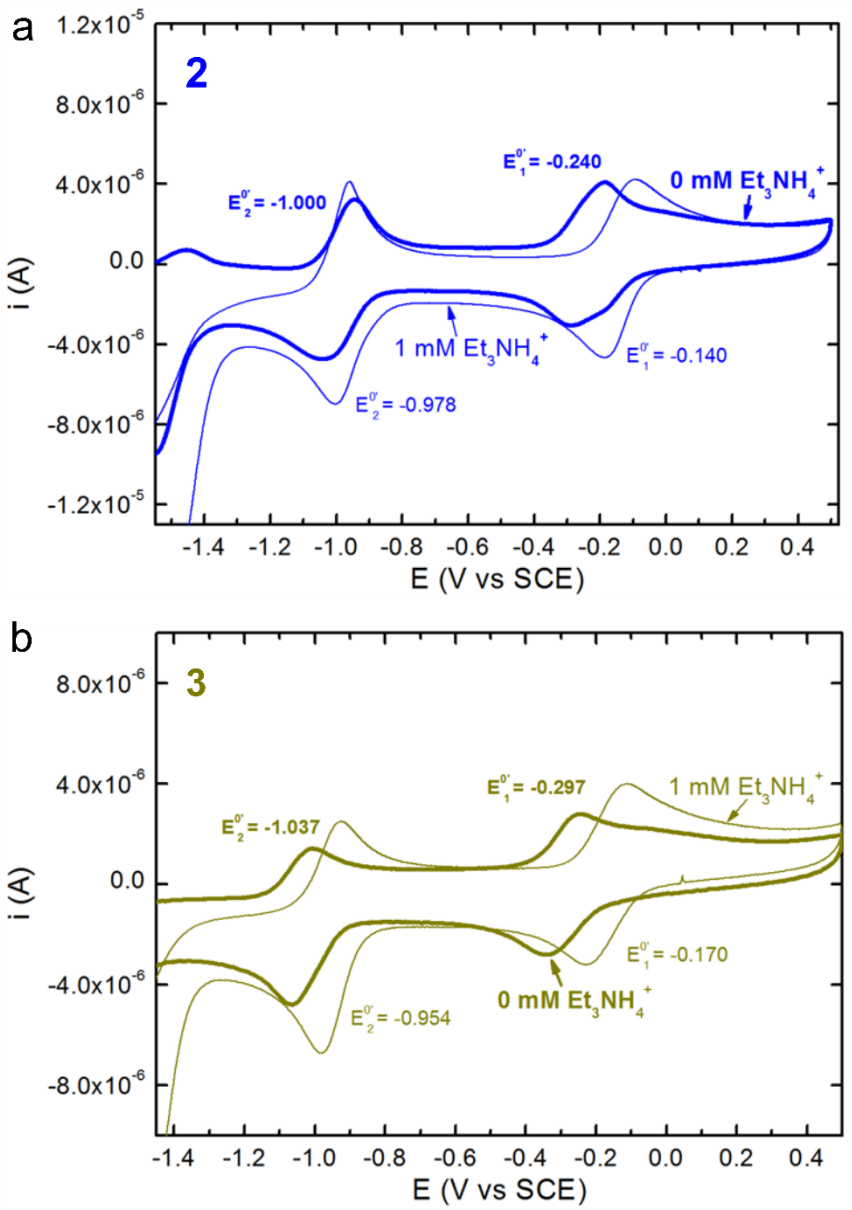

Figure S4. CVs of 0.5 mM **2** (a) and **3** (b) in the absence (thick lines) and in the presence (thin lines) of 1 mM Et_3NHCl in DMF (0.1 M $[Bu_4N^+][PF_6^-]$) at 100 mV s^{-1}. $E^{0'}{}_1$ and $E^{0'}{}_2$ denote the apparent standard potential measured for the first and second cathodic waves, respectively.

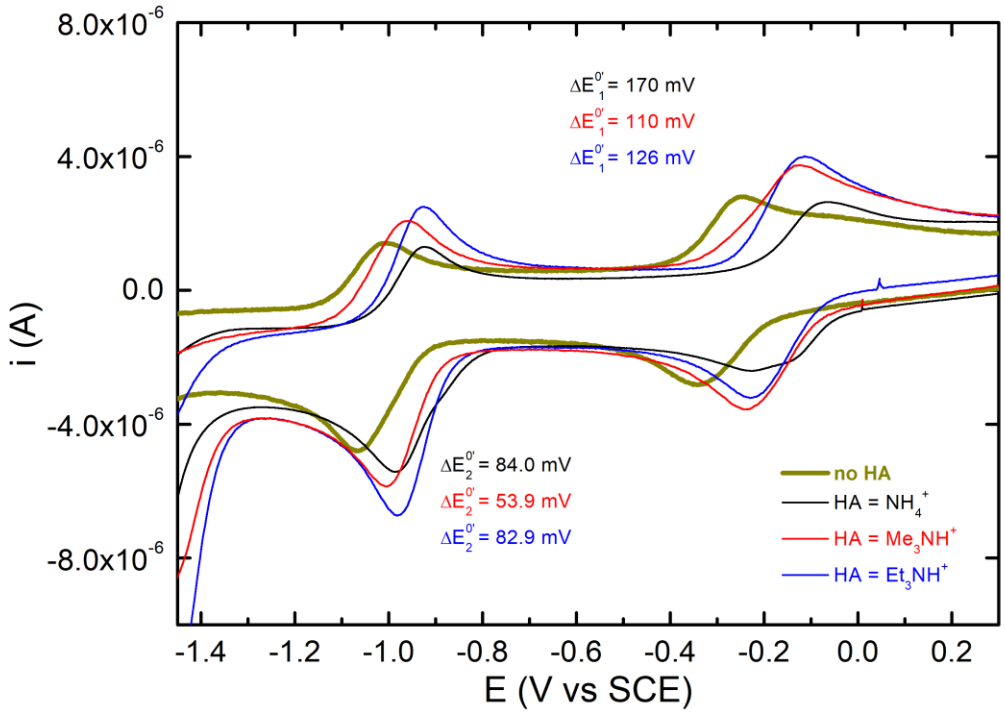

Figure S5. CVs of 0.5 mM **3** in the absence (dark yellow) and in the presence of 1 mM Me_3NHCl (red), Et_3NHCl (blue) and H_4NCl (black) in DMF (0.1 M $[Bu_4N^+][PF_6^-]$) at 100 mV s^{-1}. $\Delta E^{0'}{}_1$ and $\Delta E^{0'}{}_2$ denote the shift of apparent standard potential between CVs measured in the presence of the proton source and that measured without HA for the first and second waves, respectively.

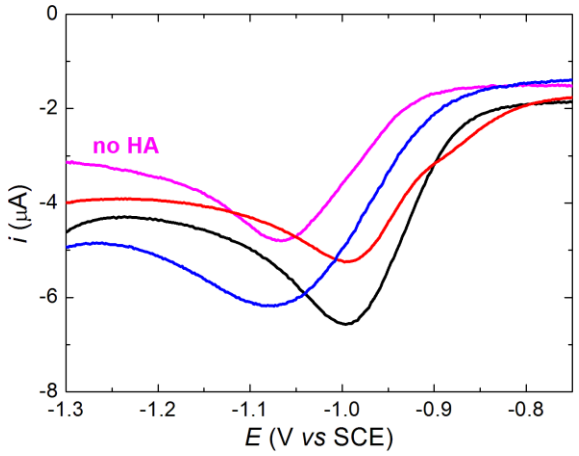

Figure S6. Cathodic waves obtained for the Fe^{II}(porphyrin)/Fe^{I}(porphyrin)$^-$ couple in the absence (pink) and in the presence of 10 mM of the different proton sources Et_3NHCl (black), NH_4Cl (red) and NH_4PF_6 (blue) in DMF (0.1 M $[Bu_4N^+][PF_6^-]$) at 100 mV s^{-1}.

S2. Detailed study of iron-based porphyrin 4.

We have here studied 0.5 mM **4** in DMF + 0.1 M Bu_4NPF_6. Glassy carbon electrode: 0.07 cm^2. The cell resistance has been compensated by positive feedback (476 ohm) and all the shown CVs are corrected for the ohmic drop. The addition of electrolyte (0.3 M) has no significant effect on both the position and the shape of the cyclic voltammograms (except that the compensated cell resistance is smaller: 203 ohm).

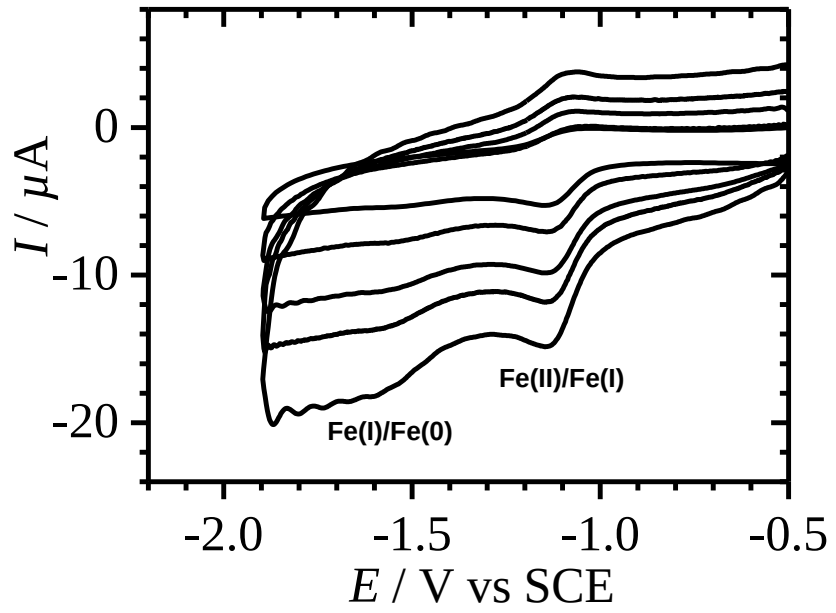

Figure S7. Cyclic voltammograms at 0.1, 0.2, 0.4, 0.6 and 1 V/s of **4** (0.5 mM) at a glassy carbon disk electrode (0.07 cm^2) in DMF + 0.1 M Bu_4NPF_6.

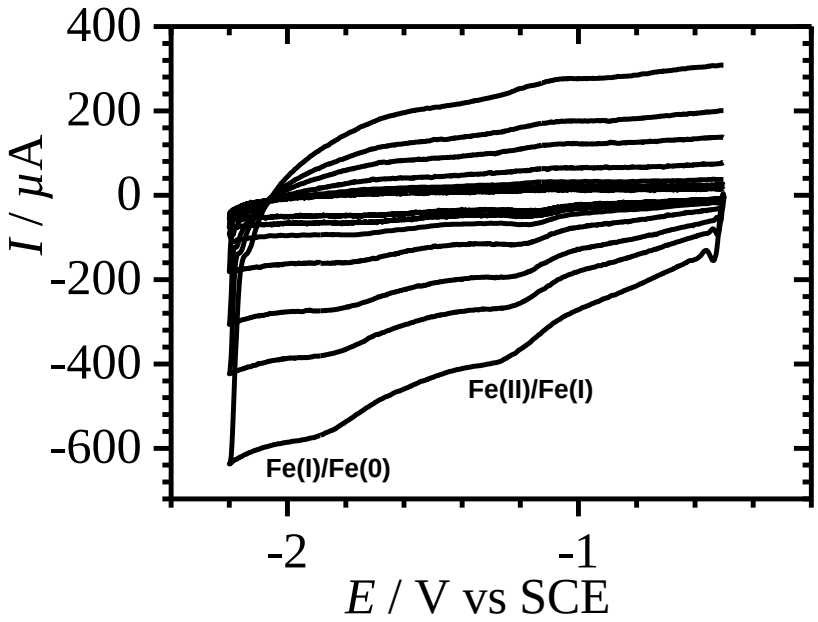

Figure S8. Cyclic voltammograms at 4, 6, 10, 20, 40, 60 and 100 V/s of **4** (0.5 mM) at a glassy carbon disk electrode (0.07 cm^2) in DMF + 0.1 M Bu_4NPF_6.

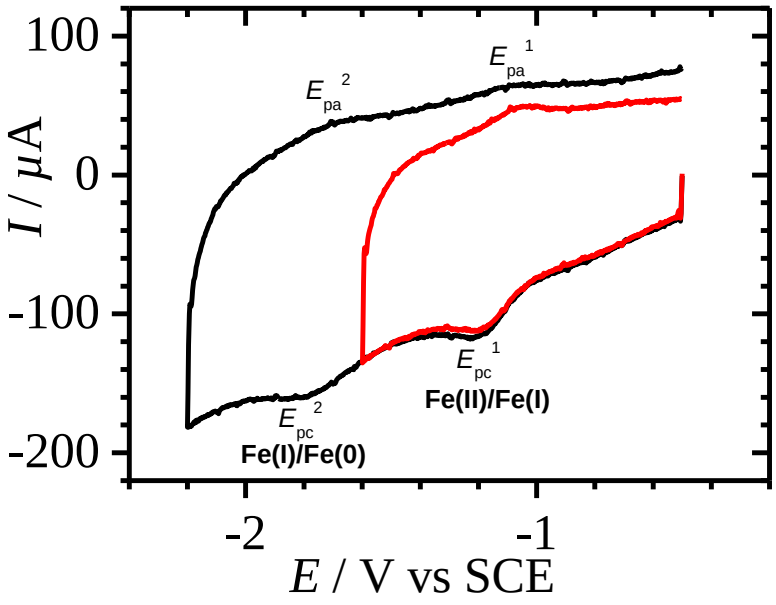

Figure S9. Cyclic voltammograms at 20 V/s of **4** (0.5 mM) at a glassy carbon disk electrode (0.07 cm^2) in DMF + 0.1 M Bu_4NPF_6. These CVs show the electrochemical reversibility of both reduction waves at high scan rates.

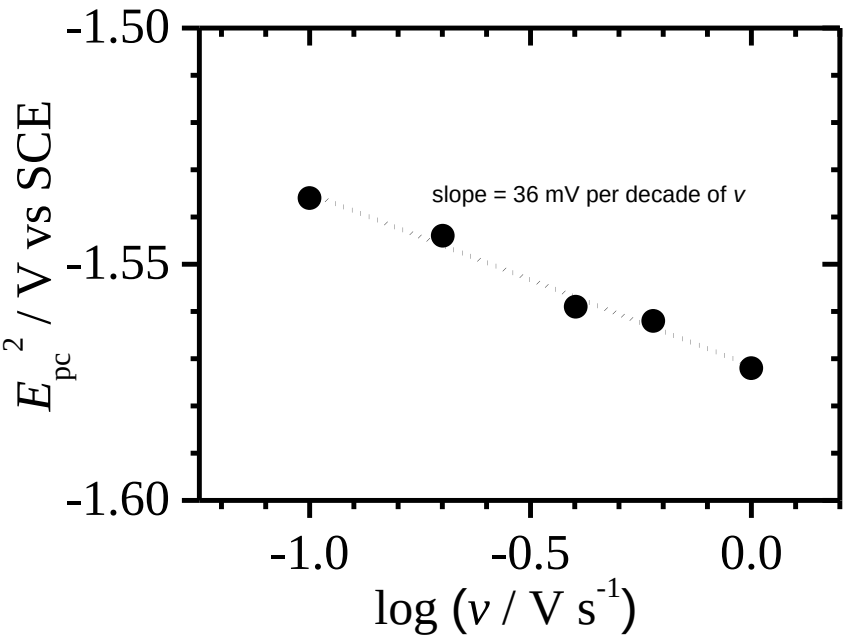

Figure S10. Variation of E_{pc} of the Fe(I)/Fe(0) reduction wave as a function of the log of the potential scan rate v in DMF + 0.1 M Bu_4NPF_6. The slope of 36 mV per decade of v is close to that theoretically expected (30 mV per decade of v) for a one-electron reversible electron transfer step (E) followed by an irreversible chemical step (C).[1]

Table S1. Determination of the apparent electron transfer rate constants k_s corresponding to the two Fe(II)/Fe(I) (process 1) and Fe(I)/Fe(0) (process 2) reduction waves. k_s was determined from the separation between the anodic and cathodic peak potentials (ΔE_p) using the Nicholson's formalism.[2]

v / V s^{-1}	ΔE_p^1 / mV	ΔE_p^2 / mV	k_s^1 / cm s^{-1}	k_s^2 / cm s^{-1}
20	107	105	0.07	0.08
39.6	138	120	0.06	0.08
60	153	175	0.06	0.04
99.5	174	218	0.05	0.04

$$k_s = \psi \left(D\pi \frac{nFv}{RT} \right)^{1/2}$$

where D is the diffusion coefficient of **4** (assumed to be equal to 10^{-5} cm^2 s^{-1}), n is the number of exchanged electrons (n = 1 for both systems), F is the Faraday's constant, R is the gas constant, T is temperature (293 K) and v is the potential scan rate (in V s^{-1}). Ψ is a kinetic parameter which is directly correlated to ΔE_p.

Average values of 0.06 cm s^{-1} were obtained for both reduction waves.

Table S2. Values of the apparent standard potentials ($E^{0'}$) and separation between the anodic and cathodic peak potentials (ΔE_p) for the successive redox waves corresponding to Fe^{III}(porphyrin)$^+$/Fe^{II}(porphyrin), Fe^{II}(porphyrin)/Fe^{I}(porphyrin)$^-$ and Fe^{I}(porphyrin)$^-$/Fe^{0}(porphyrin)$^{2-}$ for all catalyst studied in this research, based on the voltammograms of Figure 2.

	Fe^{III}(porphyrin)$^+$/Fe^{II}(porphyrin)		Fe^{II}(porphyrin)/Fe^{I}(porphyrin)$^-$		Fe^{I}(porphyrin)$^-$/Fe^{0}(porphyrin)$^{2-}$	
	$E^{0'}$(V *vs* SCE)	ΔE_p (V)	$E^{0'}$(V *vs* SCE)	ΔE_p (V)	$E^{0'}$(V *vs* SCE)	ΔE_p (V)
1	-0.15	0.12	-1.02	0.06	-1.64	0.06
2	-0.24	0.10	-0.99	0.09	-1.51	0.10
3	-0.29	0.10	-1.04	0.06	nc	nc
4	-0.21	0.14	-1.10	0.10	nc	nc
2'	-0.09	0.08	-0.94	0.06	-1.51	0.09
3'	-0.12	0.08	-0.97	0.07	-1.53	0.05
4'	-0.15	0.13	-1.06	0.07	-1.67	0.11

S3. UV-vis titration studies of 1-4 and 2'-4' with Et_3NHCl

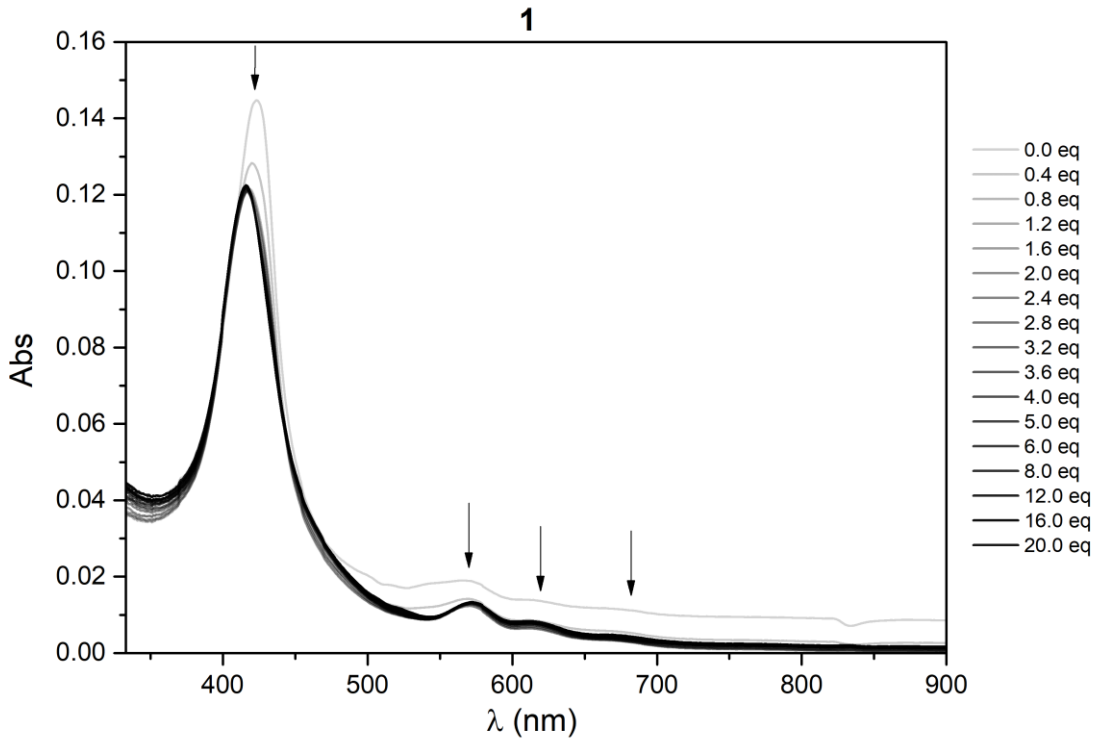

Figure S11. UV-vis spectra of **1** (1 μM) as a function of the increasing equivalent number of Et_3NHCl (from 0.0 to 20.0 equivalent).

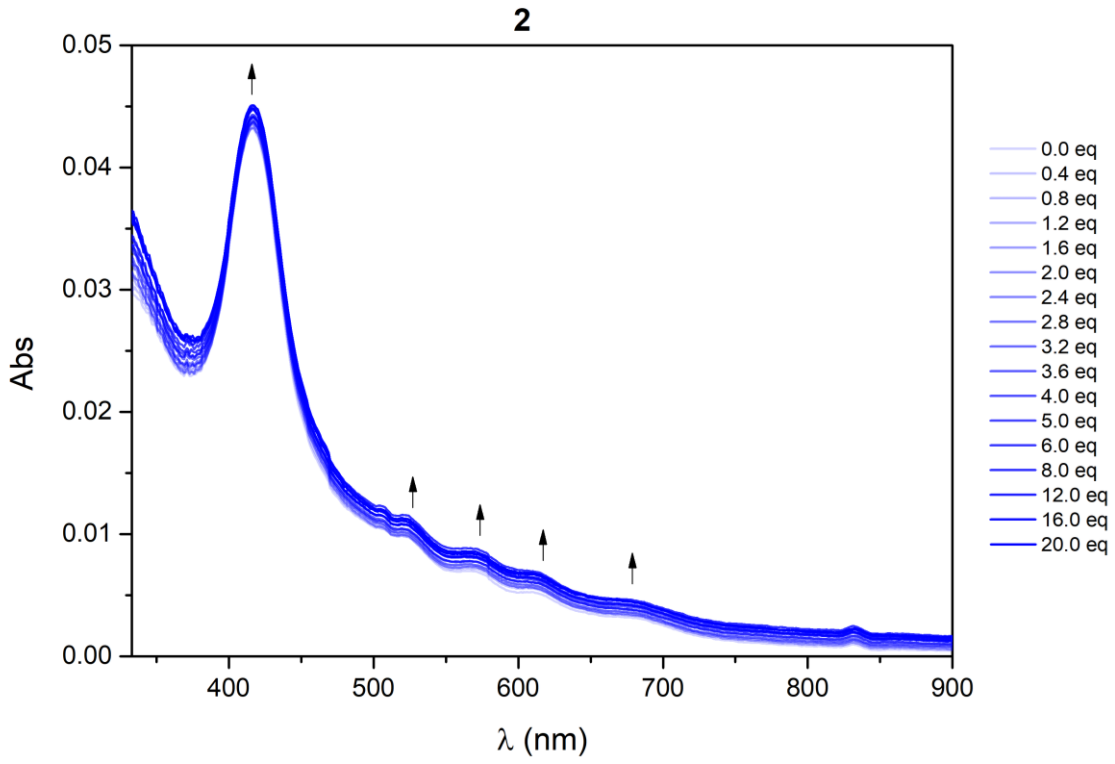

Figure S12. UV-vis spectra of **2** (1 μM) as a function of the increasing equivalent number of Et_3NHCl (from 0.0 to 20.0 equivalent).

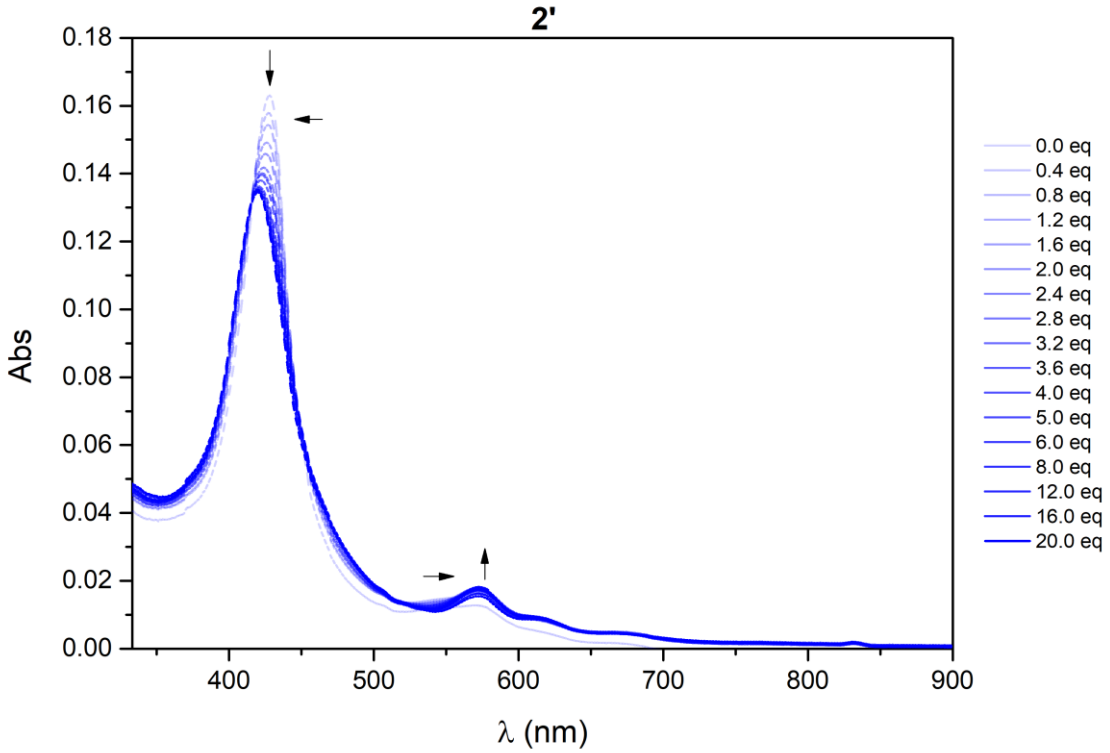

Figure S13. UV-vis spectra of **2'** (1 μM) as a function of the increasing equivalent number of Et_3NHCl (from 0.0 to 20.0 equivalent).

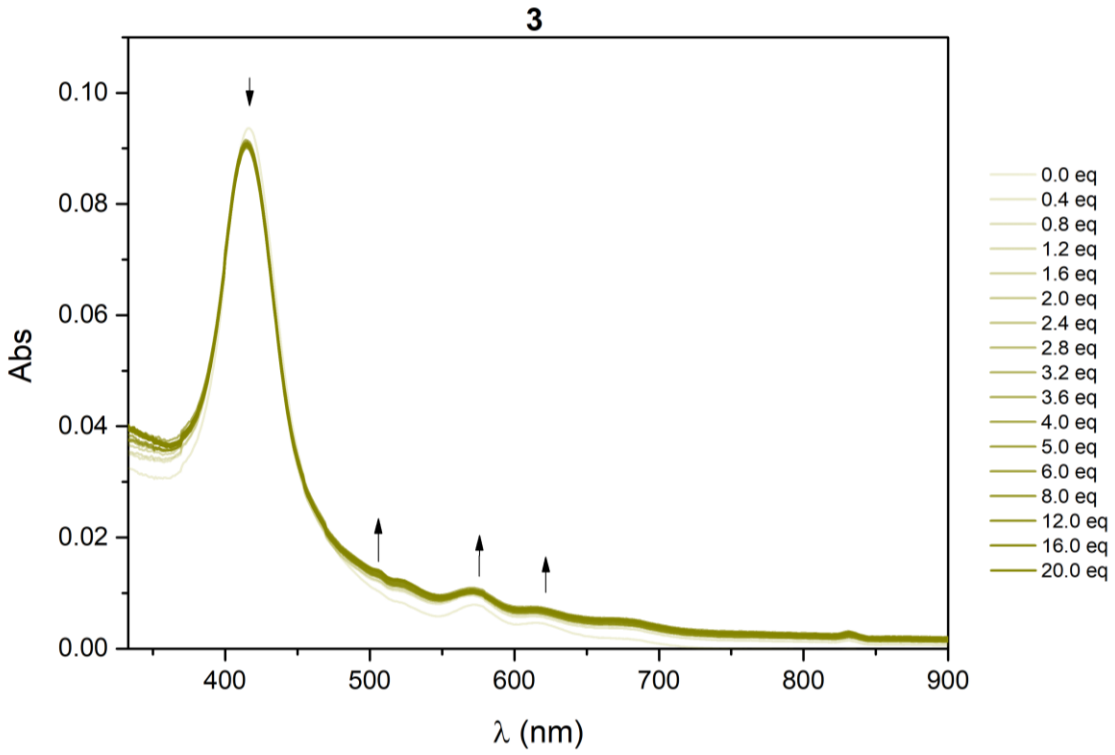

Figure S14. UV-vis spectra of **3** (1 μM) as a function of the increasing equivalent number of Et_3NHCl (from 0.0 to 20.0 equivalent).

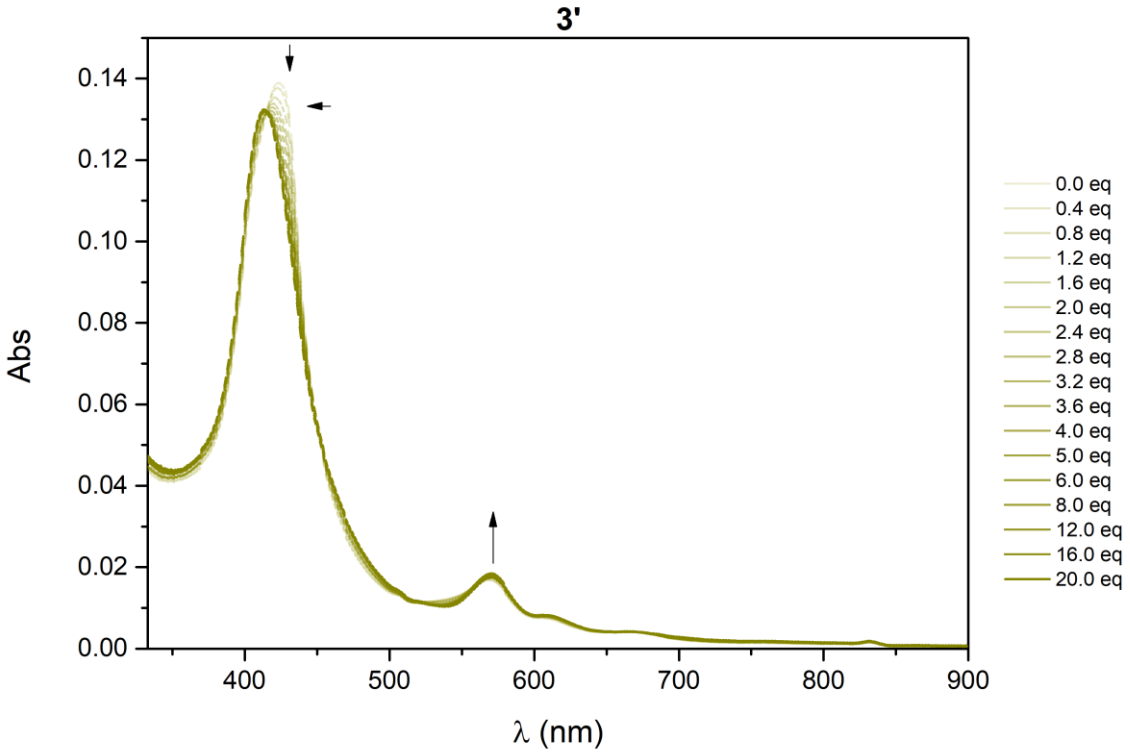

Figure S15. UV-vis spectra of **3'** (1 μM) as a function of the increasing equivalent number of Et_3NHCl (from 0.0 to 20.0 equivalent).

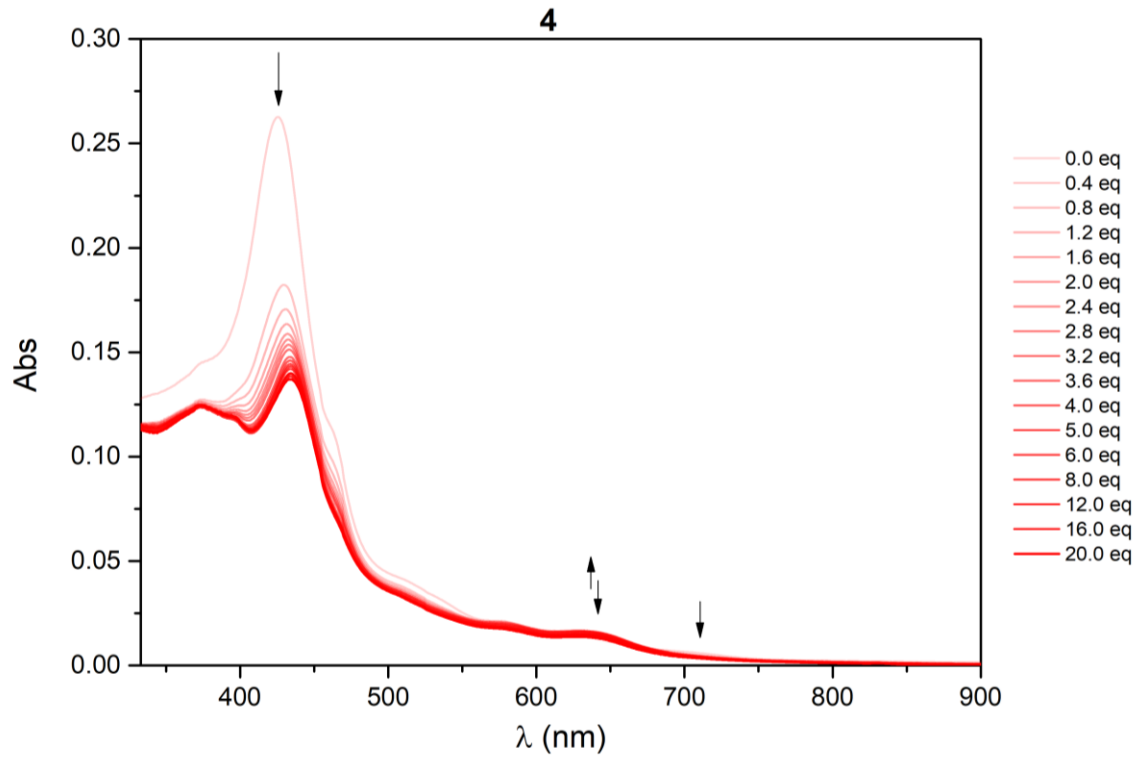

Figure S16. UV-vis spectra of **4** (10 μM) as a function of the increasing equivalent number of Et_3NHCl (from 0.0 to 20.0 equivalent).

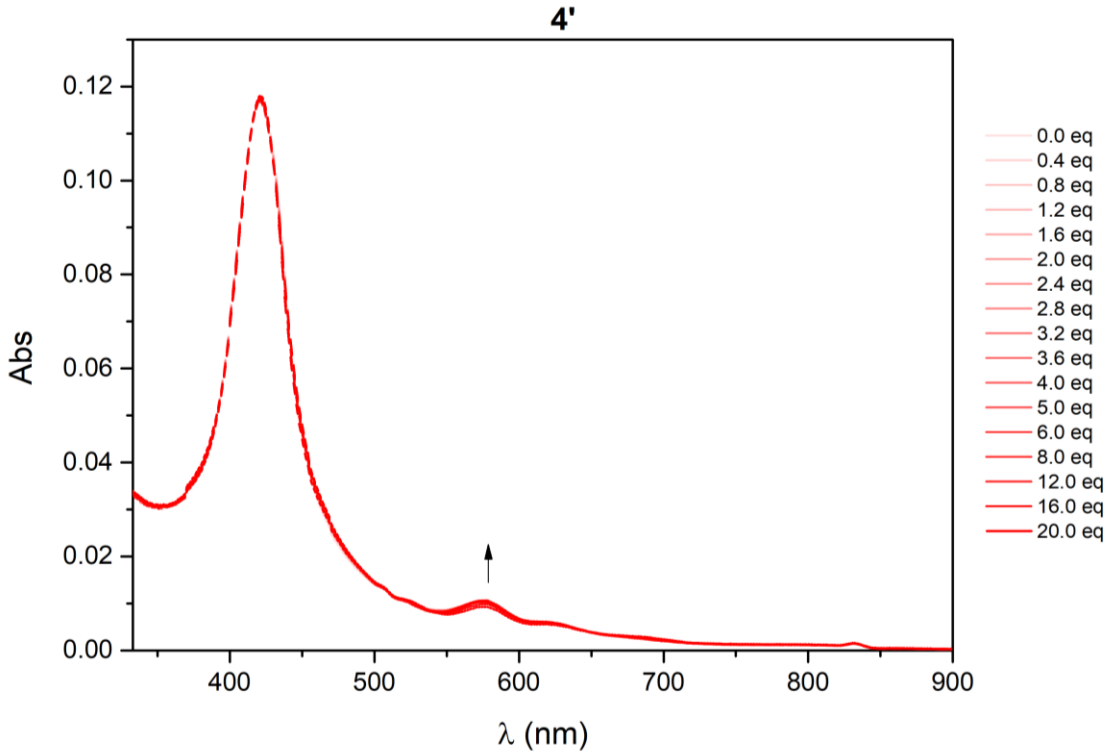

Figure S17. UV-vis spectra of **4'** (1 μM) as a function of the increasing equivalent number of Et_3NHCl (from 0.0 to 20.0 equivalent).

S4. Computational Study

Molecular modeling calculations were performed using PM3-Spartan molecular modeling program.

S4.1. XYZ cartesian coordinates for the molecular modelled structure 4* + Cl.

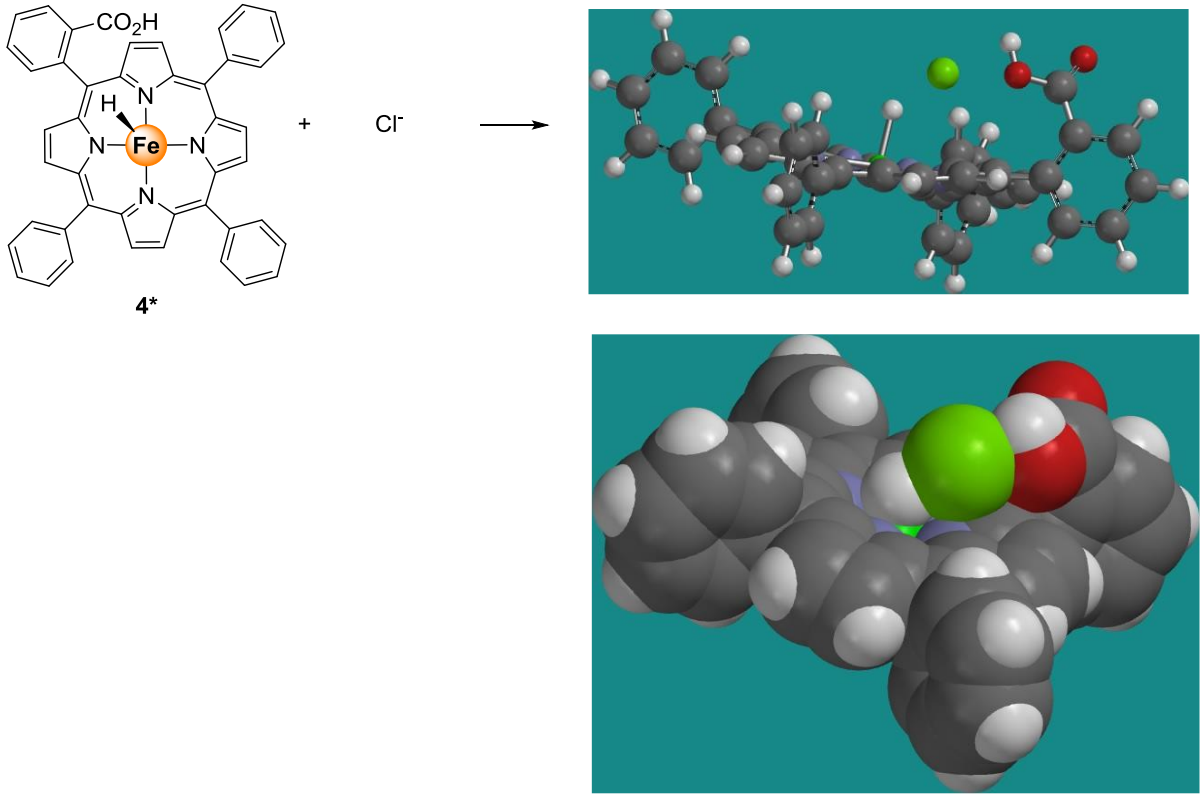

Figure S18.

C	-3.157271	-2.300694	-3.248892
C	-3.049678	-3.277409	-2.249281
C	-2.594650	-1.125926	-2.768207
C	-2.453550	-2.694943	-1.139590
N	-2.184015	-1.392892	-1.483346
H	-3.583297	-2.443368	-4.234772
H	-3.390426	-4.303310	-2.321122
C	-2.190032	-3.284340	0.128914
C	-2.419331	0.109207	-3.456876
C	-2.457680	-4.745429	0.309597
C	-2.950006	-7.481921	0.628623
C	-1.429177	-5.676726	0.108238
C	-3.737175	-5.197324	0.665465
C	-3.979991	-6.562195	0.825634
C	-1.676321	-7.040760	0.269598
C	-2.967442	0.237816	-4.843722
C	-4.006604	0.466720	-7.432188
C	-4.252282	0.761439	-5.045662
C	-2.210380	-0.177478	-5.949402
C	-2.729820	-0.060637	-7.239331

C	-4.767843	0.876404	-6.337459
H	-0.434203	-5.339455	-0.174132
H	-0.875347	-7.758780	0.113889
H	-3.140647	-8.544939	0.753092
H	-4.972549	-6.907703	1.102693
H	-4.545213	-4.485240	0.817974
H	-4.853342	1.079046	-4.196455
H	-5.764229	1.283357	-6.489297
H	-4.410616	0.555827	-8.437561
H	-2.139439	-0.382775	-8.093195
C	-1.730355	1.164271	-2.981566
C	-1.779060	-2.604202	1.215841
H	-1.215309	-0.592720	-5.805733
C	-1.422629	2.359801	-3.748048
C	-0.656840	3.184677	-3.037138
C	-0.535726	2.494587	-1.743048
N	-1.165447	1.324318	-1.773535
H	-1.730820	2.551977	-4.763372
H	-0.248159	4.132998	-3.330994
C	-1.664522	-3.176476	2.546406
C	-1.322319	-2.239470	3.427258
C	-1.165020	-1.038699	2.590757
N	-1.435090	-1.309474	1.317453
H	-1.852431	-4.205767	2.806648
H	-1.168320	-2.341615	4.485244
C	-0.698225	0.208593	3.190306
C	0.141631	3.146178	-0.624390
C	0.804618	4.459812	-0.805827
C	1.956920	7.021910	-0.997792
C	0.006278	5.617747	-0.748486
C	2.194573	4.606424	-0.970247
C	2.764882	5.886161	-1.051019
C	0.578577	6.887463	-0.850481
C	-0.485921	0.303105	4.650223
C	-0.091449	0.492910	7.413977
C	0.750873	-0.041809	5.213187
C	-1.523191	0.743369	5.482583
C	-1.324767	0.837256	6.860955
C	0.945782	0.053545	6.591704
H	-1.071360	5.531391	-0.614415
H	2.404085	8.010851	-1.066474
H	-2.488801	1.012004	5.059472
H	1.564203	-0.386660	4.577686
H	-2.132740	1.178217	7.503166
H	0.061352	0.566233	8.487846
H	1.906404	-0.215412	7.023454

C	0.049930	2.570509	0.582250
C	-0.389815	1.221447	2.370265
N	-0.505646	1.365416	0.993980
C	0.240960	2.450489	2.848782
C	0.530659	3.224229	1.799552
H	1.016044	4.185324	1.861696
H	0.473043	2.687585	3.875341
H	-0.052673	7.771956	-0.804126
Fe	-1.280036	0.007146	-0.216493
H	3.842638	5.997338	-1.156773
C	3.128731	3.463628	-1.017643
O	4.201118	3.405979	-0.445496
O	2.708215	2.500554	-1.850550
H	3.376972	1.789707	-1.774519
H	0.234564	-0.521740	-0.339566
Cl	1.746051	0.432183	-1.211038

S4.2. XYZ cartesian coordinates for the molecular modelled structure 3* + $HNMe_3Cl$.

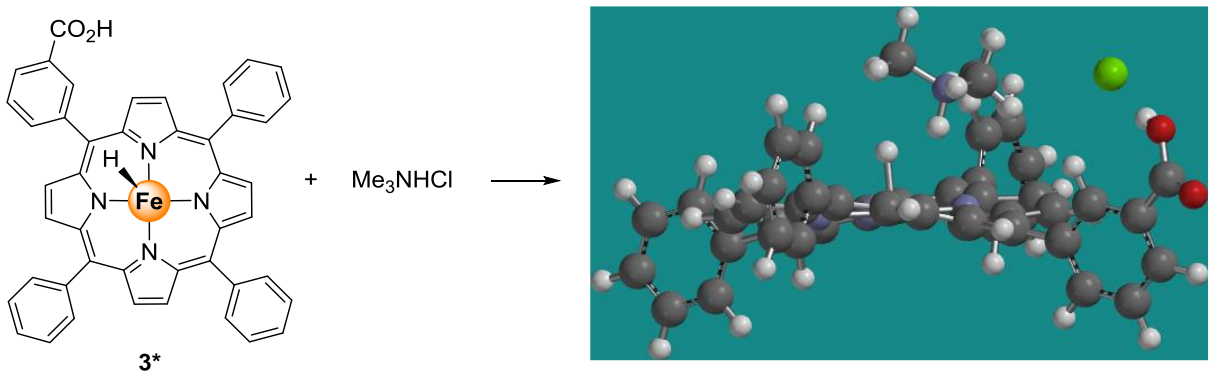

Figure S19.

C	-1.836	-2.346	-3.522
C	-2.394	-3.240	-2.598
C	-1.506	-1.179	-2.848
C	-2.368	-2.640	-1.347
N	-1.824	-1.390	-1.524
H	-1.728	-2.519	-4.586
H	-2.772	-4.232	-2.817
C	-2.792	-3.188	-0.102
C	-1.023	0.044	-3.403
C	-3.564	-4.468	-0.098
C	-5.027	-6.854	-0.103
C	-2.901	-5.705	-0.091
C	-4.965	-4.438	-0.113
C	-5.693	-5.628	-0.115
C	-3.633	-6.893	-0.092

C	-0.835	0.138	-4.884
C	-0.494	0.310	-7.657
C	-1.910	0.502	-5.710
C	0.409	-0.151	-5.463
C	0.577	-0.062	-6.846
C	-1.737	0.590	-7.091
H	-1.814	-5.744	-0.084
H	-3.116	-7.850	-0.085
H	-5.596	-7.780	-0.105
H	-6.779	-5.600	-0.125
H	-5.493	-3.486	-0.124
H	-2.885	0.719	-5.278
H	-2.572	0.876	-7.726
H	-0.362	0.378	-8.735
H	1.542	-0.286	-7.294
C	-0.820	1.172	-2.698
C	-2.458	-2.675	1.098
H	1.248	-0.453	-4.844
C	-0.519	2.471	-3.272
C	-0.516	3.408	-2.324
C	-0.748	2.640	-1.090
N	-0.910	1.349	-1.370
H	-0.386	2.681	-4.322
H	-0.373	4.467	-2.438
C	-2.695	-3.323	2.375
C	-2.121	-2.631	3.358
C	-1.564	-1.460	2.661
N	-1.807	-1.529	1.355
H	-3.226	-4.250	2.520
H	-2.104	-2.852	4.409
C	-0.926	-0.386	3.421
C	-0.697	3.298	0.216
C	-0.574	4.770	0.337
C	-0.368	7.551	0.625
C	-1.672	5.523	0.779
C	0.627	5.428	0.035
C	0.739	6.813	0.188
C	-1.569	6.908	0.923
C	-0.688	-0.535	4.872
C	-0.221	-0.804	7.618
C	0.543	-1.018	5.334
C	-1.683	-0.187	5.796
C	-1.449	-0.322	7.165
C	0.774	-1.151	6.704
H	-2.615	5.033	1.016
H	-0.296	8.633	0.721

H	-2.643	0.193	5.453
H	1.328	-1.289	4.633
H	-2.222	-0.049	7.879
H	-0.037	-0.905	8.685
H	1.732	-1.522	7.061
C	-0.664	2.507	1.299
C	-0.694	0.770	2.785
N	-0.841	1.135	1.452
C	-0.288	1.985	3.486
C	-0.318	3.009	2.628
H	-0.058	4.028	2.878
H	-2.425	7.486	1.263
H	1.471	4.862	-0.338
C	1.962	7.551	-0.208
O	3.126	6.899	-0.046
O	1.894	8.675	-0.684
H	3.162	6.081	0.527
Fe	-1.344	-0.105	-0.002
H	0.135	-0.727	-0.044
Cl	3.811	4.231	1.451
H	-0.035	2.067	4.533
N	2.398	0.969	-0.927
H	1.374	1.077	-1.028
C	2.673	0.945	0.553
C	3.003	2.190	-1.559
C	2.824	-0.283	-1.605
H	2.537	-0.218	-2.657
H	2.523	3.066	-1.129
H	2.167	1.796	1.002
H	2.253	0.021	0.960
H	2.308	-1.125	-1.135
H	4.082	2.183	-1.384
H	3.754	0.968	0.711
H	3.908	-0.389	-1.504
H	2.789	2.155	-2.631

S5. Plausible mechanism

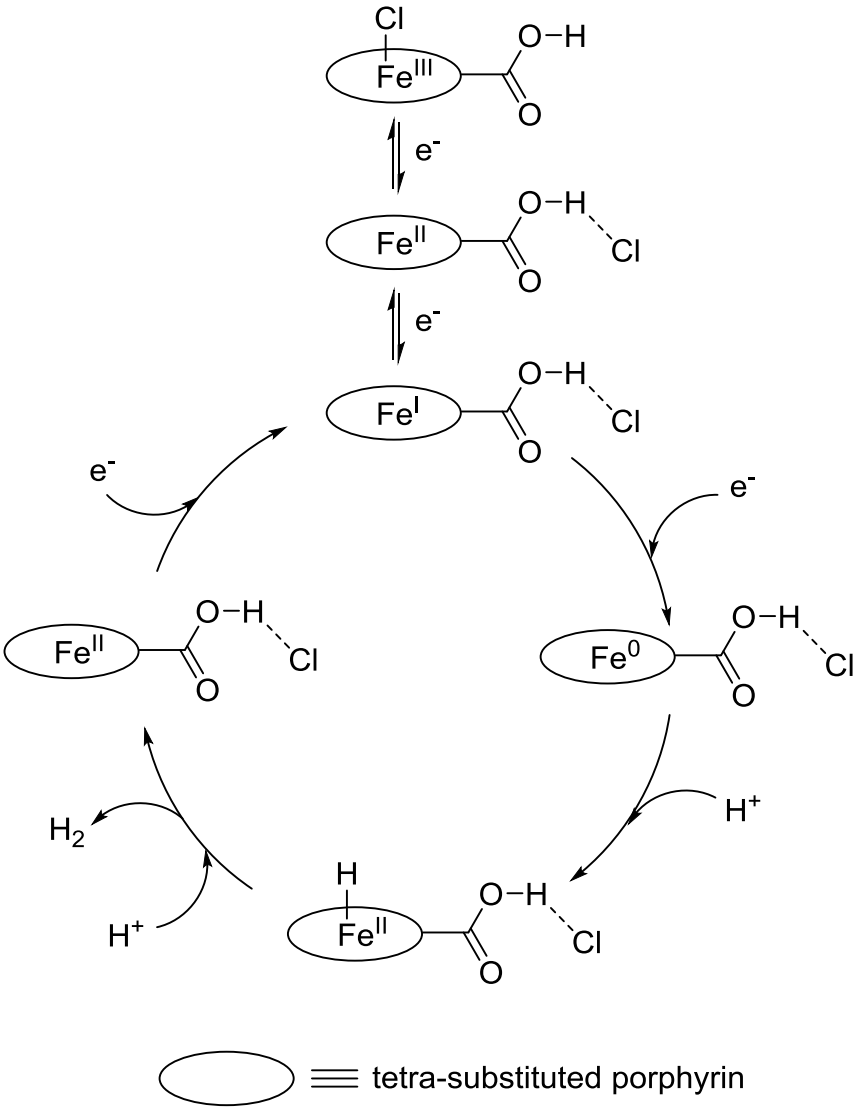

S6. NMR spectra

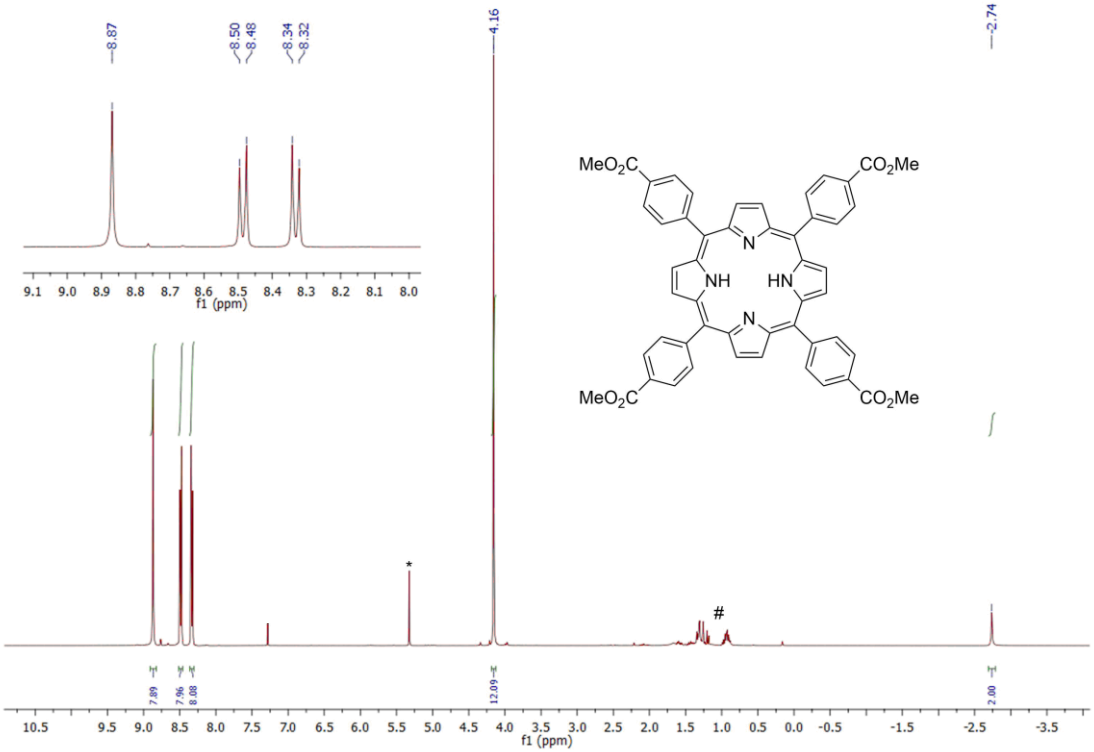

Figure S20. ^{1}H NMR (400 MHz, $CDCl_3$, 298 K) spectra of **2''**.
* denotes traces of dichloromethane, # denotes traces of petroleum ether.

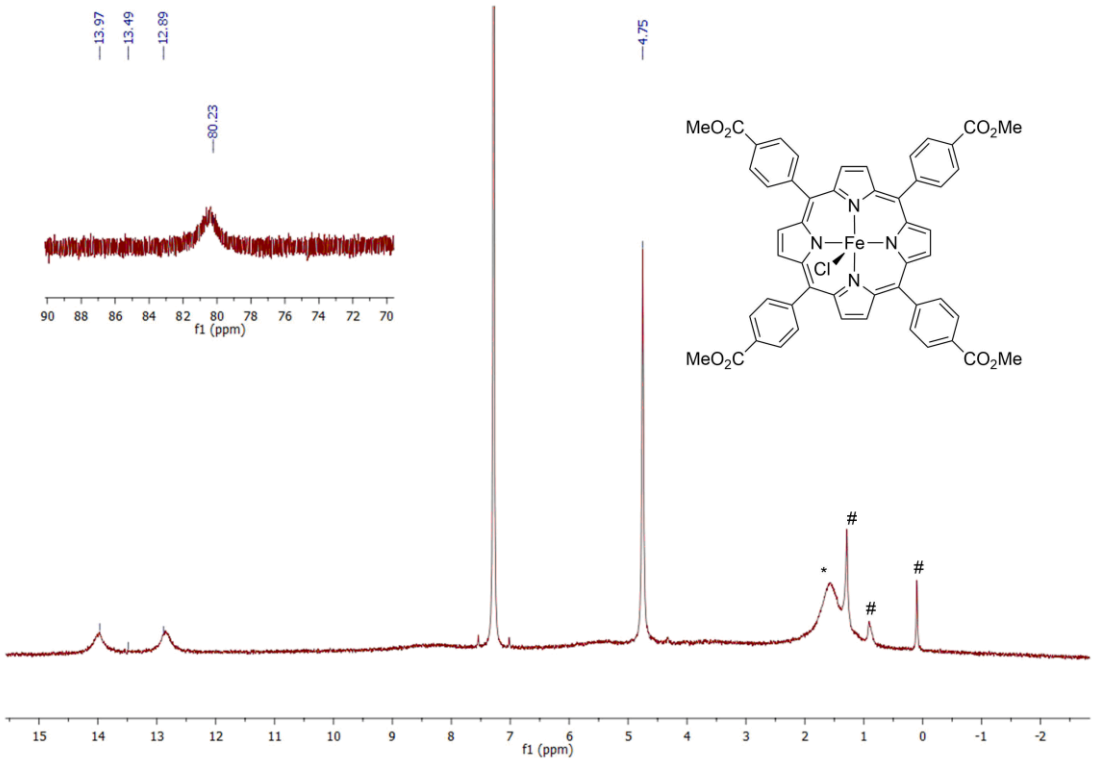

Figure S21. ^{1}H NMR (400 MHz, $CDCl_3$, 298 K) spectra of **2'**.
* denotes traces of water, # denotes traces of petroleum ether.

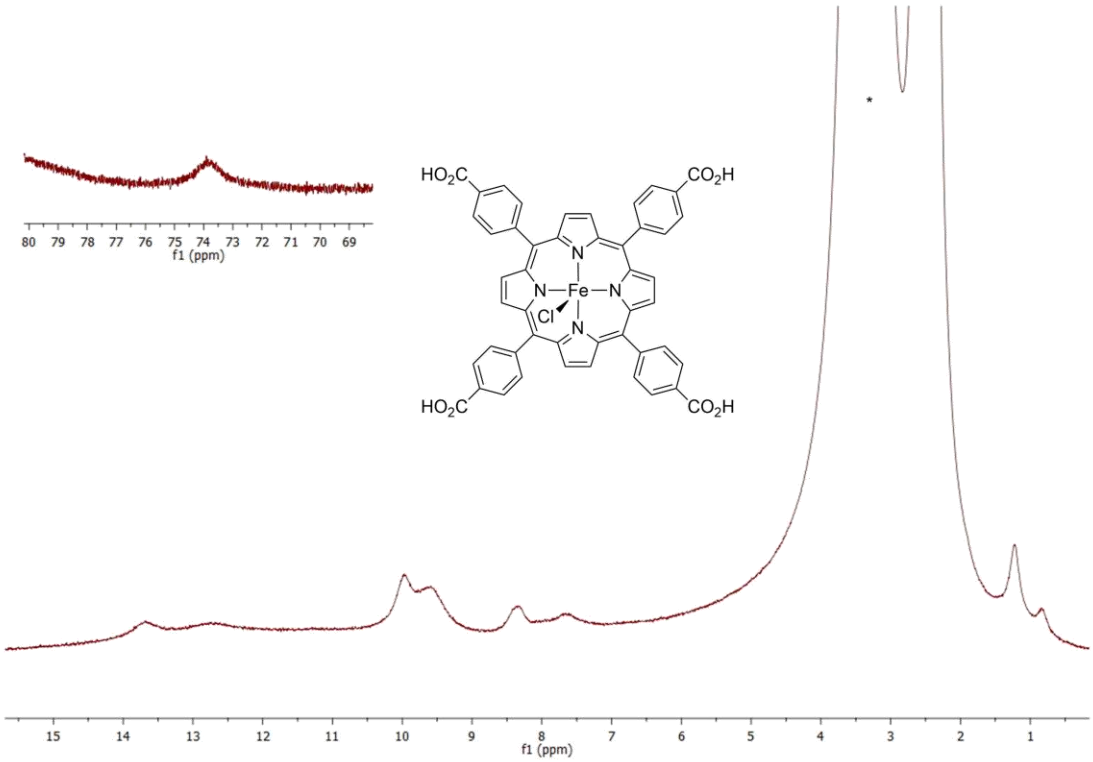

Figure S22. ^{1}H NMR (400 MHz, DMSO-d_6, 298 K) spectra of **2**.
* denotes traces of water.

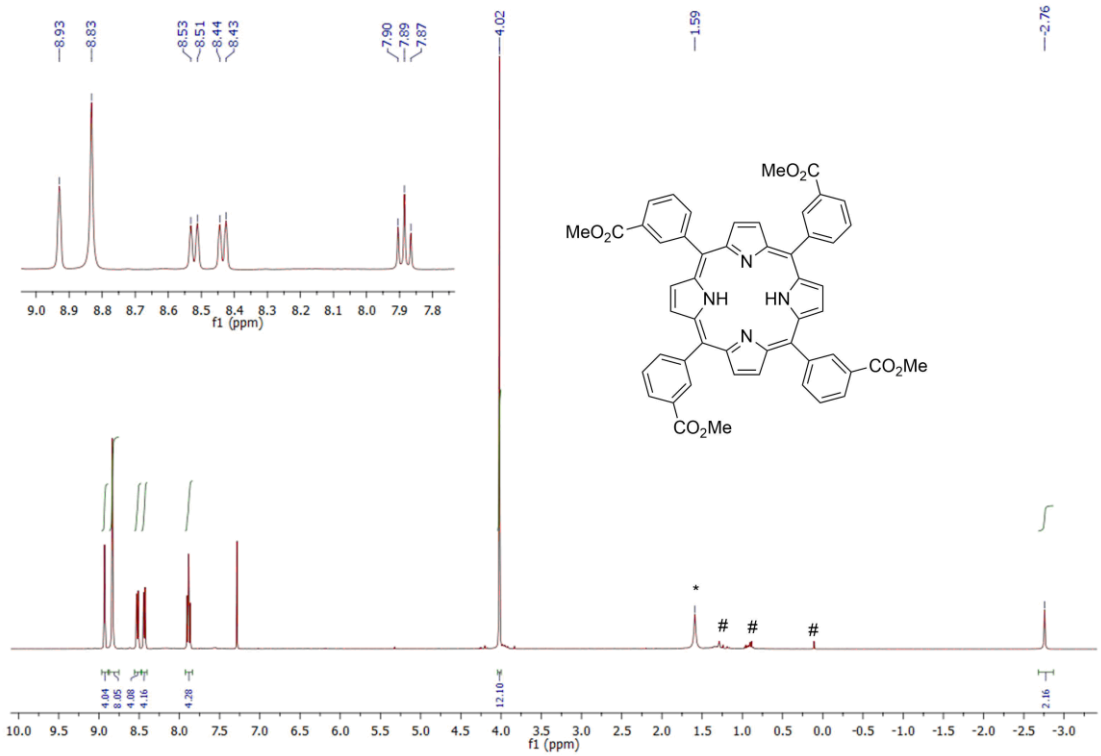

Figure S23. ^{1}H NMR (400 MHz, $CDCl_3$, 298 K) spectra of **3''**.
* denotes traces of water, # denotes traces of petroleum ether.

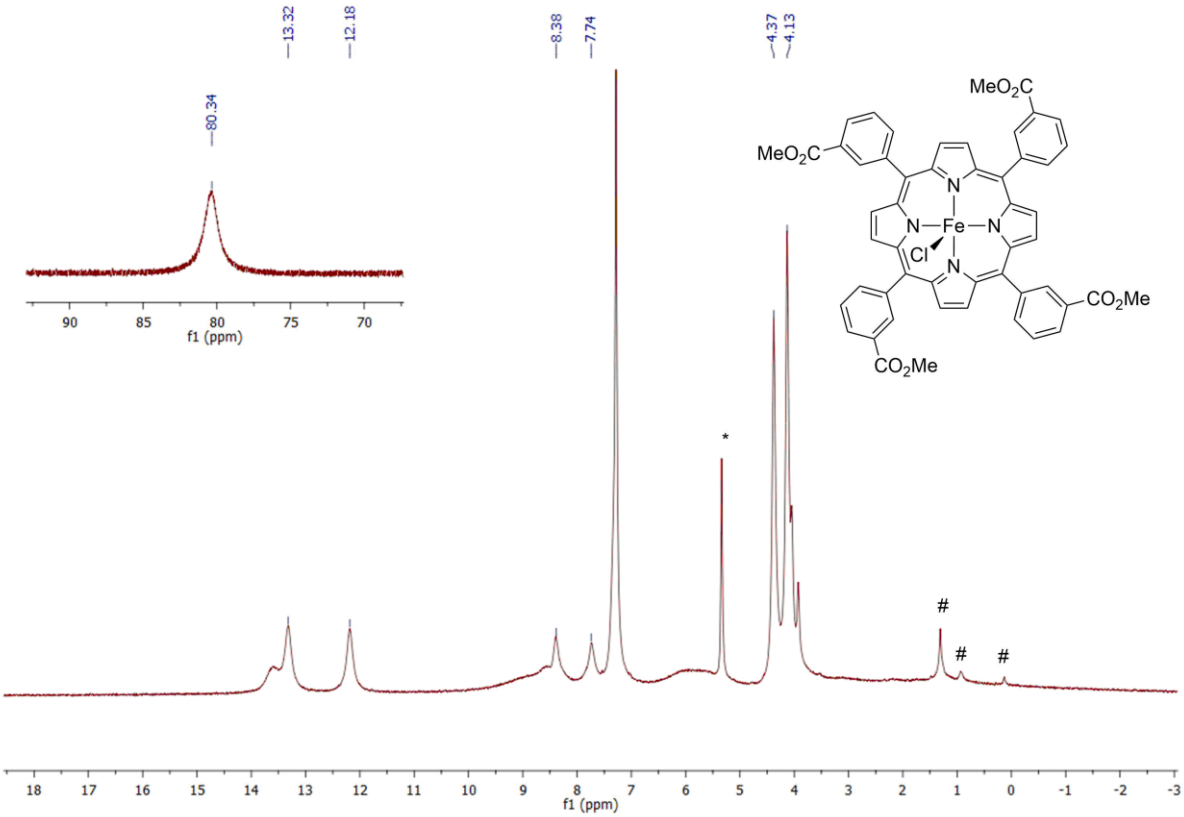

Figure S24. ^{1}H NMR (400 MHz, $CDCl_3$, 298 K) spectra of **3'**.
* denotes traces of dichloromethane, # denotes traces of petroleum ether.

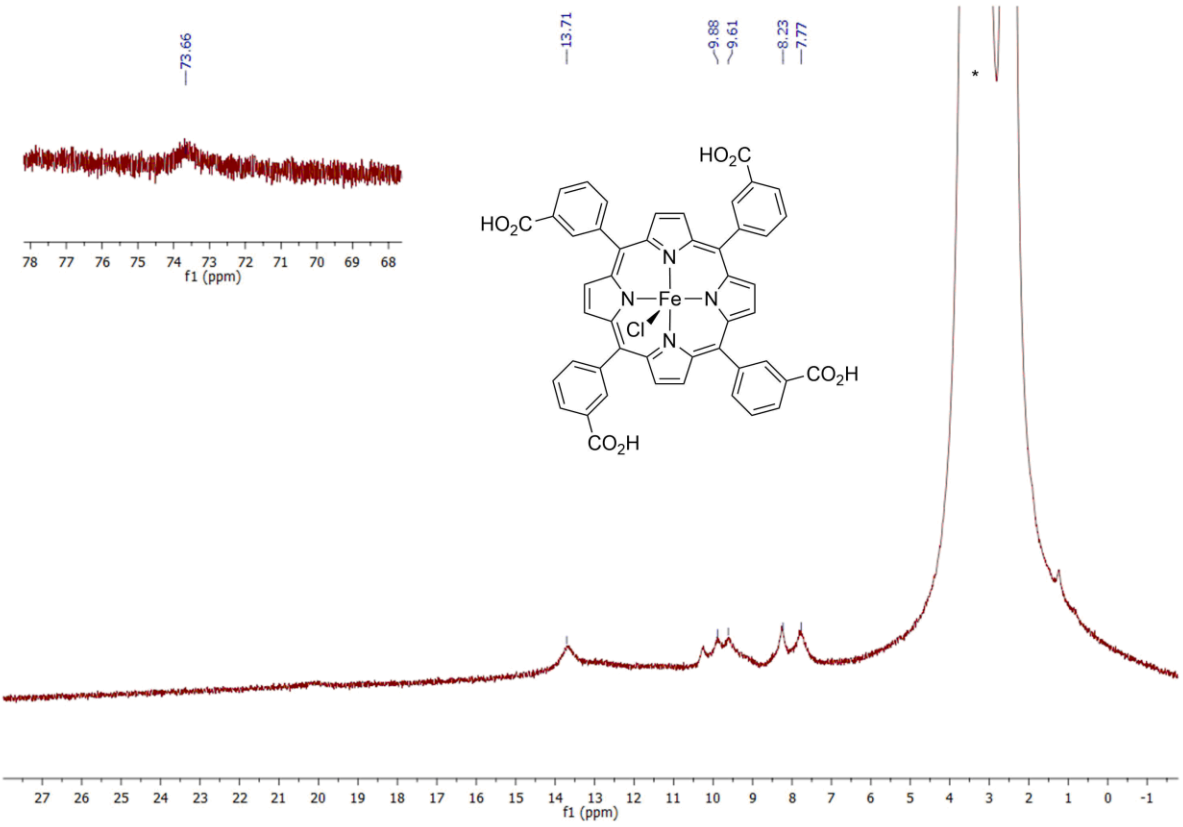

Figure S25. ^{1}H NMR (400 MHz, DMSO-d_6, 298 K) spectra of **3**.
* denotes traces of water.

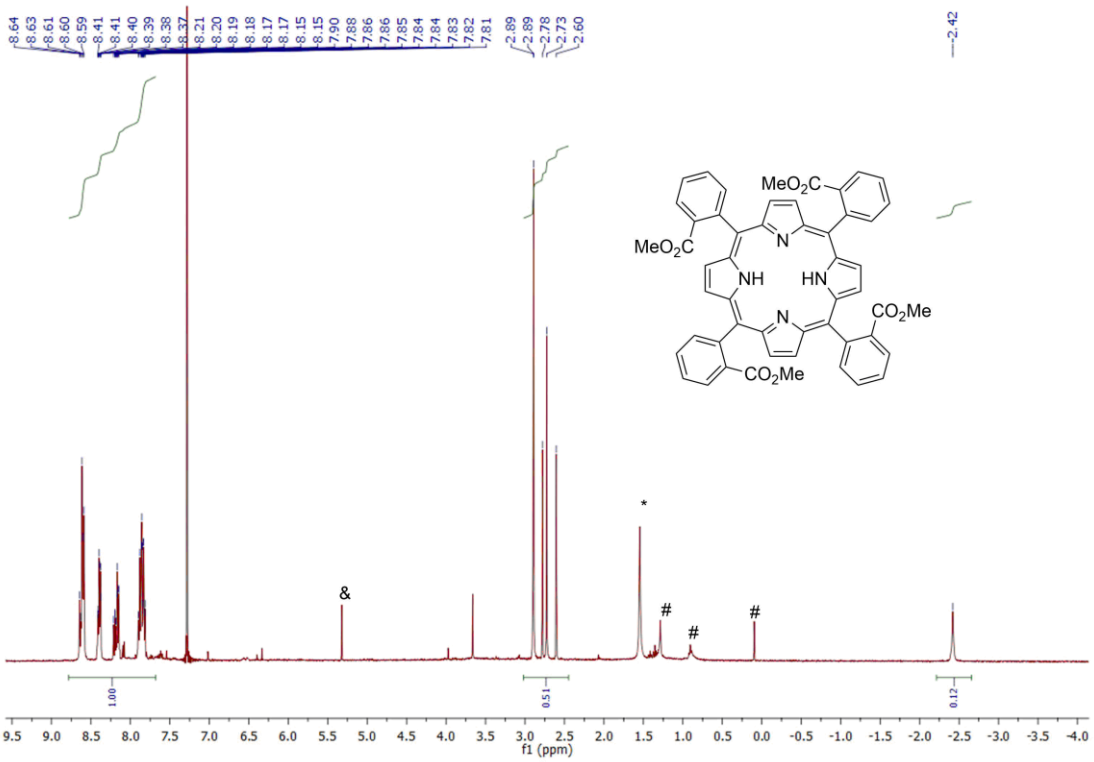

Figure S26. ^{1}H NMR (400 MHz, $CDCl_3$, 298 K) spectra of **4''**.
* denotes traces of water, # denotes traces of petroleum ether, & denotes traces of dichloromethane.

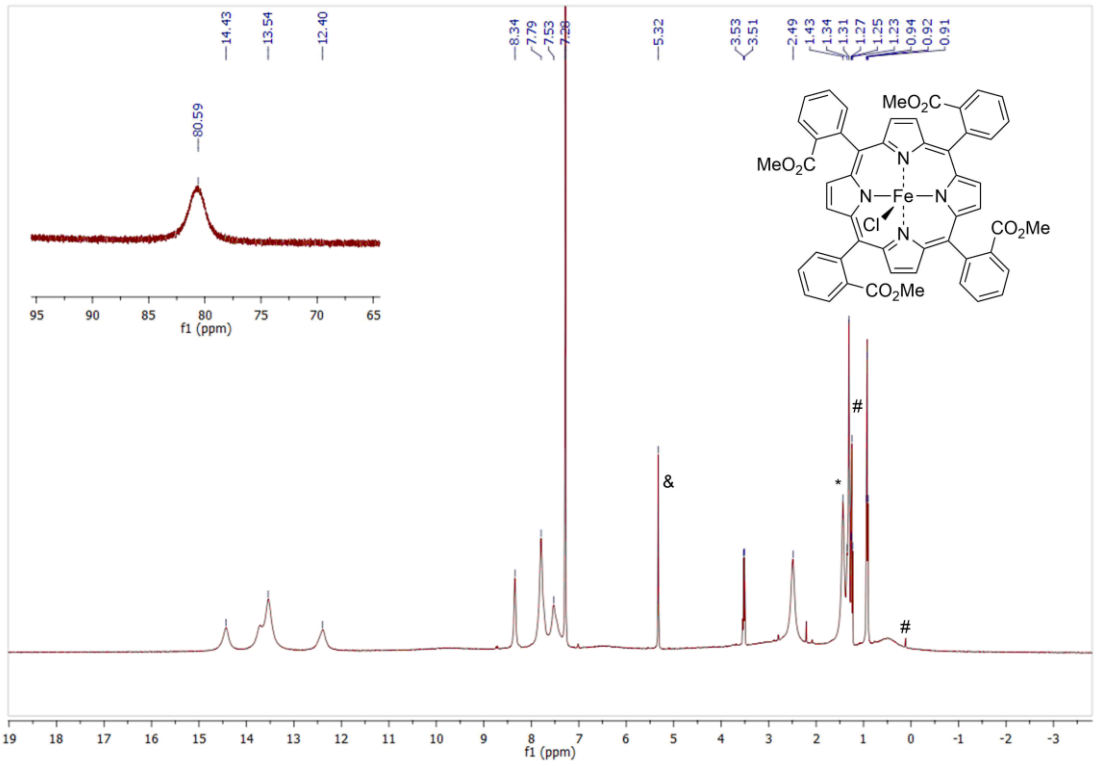

Figure S27. ^{1}H NMR (400 MHz, $CDCl_3$, 298 K) spectra of **4'**.
* denotes traces of water, & denotes traces of dichloromethane, and # denotes traces of petroleum ether.

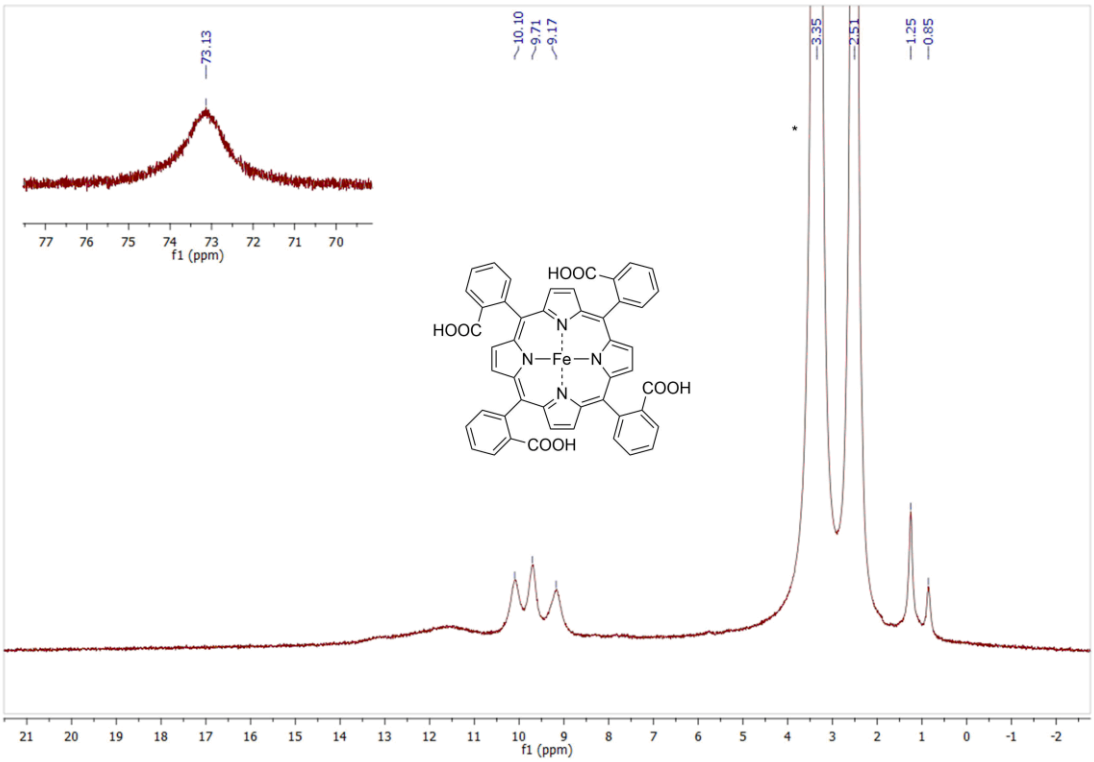

Figure S28. ^{1}H NMR (400 MHz, DMSO-d_6, 298 K) spectra of **4**.
* denotes traces of water.

S7. References

[1] Nicholson, R. S.; Shain, I. *Anal. Chem.* **1964**, *36*, 706–723.
[2] Nicholson, R. S. *Anal. Chem.* **1965**, *37*, 1351–1355.